Thermoelectric properties of cobalt–antimonide thin films prepared by radio frequency co-sputtering

Aziz Ahmed, Seungwoo Han *

Department of Nano-Mechatronics, Korea University of Science and Technology (UST), 171 Jang-dong, Yuseong-gu, Daejeon 305-343, Republic of Korea
Department of Nano-Mechanics, Korea Institute of Machinery and Materials, 171 Jang-dong, Yuseong-gu, Daejeon 305-343, Republic of Korea

ARTICLE INFO

ABSTRACT

Co–Sb thin films with an Sb content in the range 65–76 at.%, were deposited on a thermally oxidized Si (100) substrate preheated at 200 °C using radio-frequency co-sputtering. Evaluation using scanning electron microscopy images and X-ray diffraction reveals that the films were polycrystalline, with a grain size in the range 100–250 nm. Energy-dispersive spectroscopy analysis indicates single-phase $CoSb_2$ and $CoSb_3$ films, as well as multiphase thin films with either $CoSb_2$ or $CoSb_3$ as the dominant phase. The electrical and thermoelectric properties were measured and found to be strongly dependent on the observed phases and the defect concentrations. The $CoSb_2$ thin films were found to exhibit a significant n-type thermoelectric effect, which, coupled with the very low electrical resistivity, resulted in a larger power factor than that of the $CoSb_3$ thin films. We find power factors of 0.73 $mWm^{-1} K^{-2}$ and 0.67 $mWm^{-1} K^{-2}$ for the $CoSb_2$ and $CoSb_3$ thin films, respectively.

1. Introduction

Thermoelectric materials and devices are based on direct conversion of heat into electricity (the Seebeck effect) or use an externally provided current to remove heat from the system under consideration (the Peltier effect). A key parameter is the figure of merit, ZT, which defines the thermoelectric conversion efficiency and is given by

$$ZT = \frac{S^2 T}{\rho \kappa} \qquad (1)$$

where S is the Seebeck coefficient or thermoelectric power, ρ is the electrical resistivity, κ is the total thermal conductivity, and T is temperature. Existing commercially available thermoelectric materials have a figure of merit of around unity; however, the efficiency has not yet reached the level whereby these devices are suitable for widespread use, and applications remain limited to a few specific domains. To improve the efficiency, high performance semiconducting or semi-metallic thermoelectric materials are required, and there have been a number of reports of the synthesis and properties of such thermoelectric materials [1–6].

Co–Sb-based bulk and thin-film systems have been investigated for some time, with the focus on $CoSb_3$ and doped alloys thereof. This is because of the complex skutterudite cubic structure, which leads to potential thermoelectric applications at moderate temperatures. $CoSb_3$ is a narrow-band-gap semiconductor, with high charge carrier mobility, a low electrical resistivity and a relatively high Seebeck coefficient. In binary form, the unit cell contains 32 atoms arranged in 8 groups of MX_3 blocks, where M is the metal atom and X is a pnicogen atom. Six of these blocks contain planar rings of pnicogen atoms, whereas the remaining two empty blocks form voids in the skutterudite, thus providing a basis for the thermoelectric potential [1,2,7–13]. Anno et al. [14] obtained a Seebeck coefficient of $S = 600$ μV/K for 71-nm-thick p-type $CoSb_3$ films formed using radio frequency (RF) sputtering using alloy target and annealed at 750 °C. Christen et al. [15] obtained high charge carrier mobility and electrical conductivity for thin films formed using pulsed-laser deposition (PLD), and observed a p- to n-type transition in the Seebeck coefficient at elevated temperatures. Savchuk et al. [16] reported a Seebeck coefficient of $S = -250$ μV/K for 190-nm-thick n-type $CoSb_3$ films deposited using direct current (DC) sputtering and annealed at 200 °C and 350 °C. Kumar et al. [12] obtained a power factor of 0.97 $mWm^{-1} K^{-2}$ for In- and Yb-doped $CoSb_3$ films deposited using PLD thin films on a glass substrate.

Despite these achievements, obtaining $CoSb_3$ thin films with a high degree of crystallinity remains a challenge, and the thermoelectric properties of the bulk material remain superior to those of thin films [9,17]. The reasons for this are the larger defect concentration, the presence of impurity phases in the thin films, and inhomogeneities in the Sb/Co ratio, all of which adversely affect the structural and thermoelectric properties [11,18–20]. Another significant issue is the combination of these effects, which makes the temperature dependence of the thermoelectric properties complex and the results of experiments on $CoSb_3$ thin films difficult to interpret. There is, therefore, a requirement to improve the synthesis techniques and deposition environment used to form $CoSb_3$ thin films. While investigating $CoSb_2$ single crystals, Caillat

* Corresponding author at: Postal address: 104 Sinesongno, Yuseong-Gu, Daejeon, 305-343, Republic of Korea. Tel.: +82 42 868 7426; fax: +82 42 868 7884.
E-mail address: swhan@kimm.re.kr (S. Han).

[7] discovered that heavily doped semiconducting behavior was characterized by a large charge carrier mobility, leading to a large negative Seebeck coefficient of $S = -50$ μV/K at 300 °C. CoSb$_2$ thin films therefore also have potential thermoelectric applications.

In this work, we deposited Co–Sb thin films on heated substrates using RF co-sputtering. The focus was to prepare thin films with stoichiometric ratios corresponding to either CoSb$_2$ or CoSb$_3$. In addition, films with intermediate compositions were also prepared to gain insight into the effects of impurity phases (i.e., the presence of CoSb$_2$ in CoSb$_3$ films and vice versa) on the thermoelectric and charge transport properties.

2. Experimental procedure

Thin films were prepared using RF co-sputtering deposition (ATC ORION sputtering system, AJA International Inc.) with separate Co and Sb targets. The base pressure of the chamber during deposition was 1.33×10^{-5} Pa. Ar was used as the carrier gas, with pressure during deposition of 0.4 Pa. The films were deposited on thermally oxidized Si (100) substrates at a temperature of 200 °C. The substrates were first wet cleaned using alcohols and deionized water followed by plasma cleaning. The RF power applied to the Sb target was varied in the range 40–55 W and the power at the Co target was fixed at 60 W. To achieve a uniform film thickness and composition, the substrate was rotated at 10 rpm. The deposition time was 1 h, and the film thickness was in the range 400–600 nm, depending on applied RF sputtering power to the Sb target.

The atomic composition of the films was determined using energy dispersive spectroscopy (EDS) setup of Horibar X-max type with 15 kV operating voltage and 10 mA beam current. The thickness, cross-section and surface morphology were investigated using scanning electron microscopy (SEM) using Hitachi S-4800 system at 10 kV operating voltage. Ex-situ room-temperature X-ray diffraction (XRD) patterns were obtained using a Rigaku D/MAX-2500 diffractometer with Cu k$_\alpha$ radiation source, where the diffraction angle 2θ was varied in the range 20–80° with a step size of 0.01° and 40 kV operating voltage. High-temperature XRD results obtained from this system were used to calculate the lattice parameter of the films as a function of temperature.

Hall measurements were carried out at room temperature using the Van der Pau technique with a DC current of 1 mA and a magnetic field of 0.55 T to characterize the charge carrier mobility of the films, using an Ecopia HMS 5000 system. The temperature dependence of the electrical properties (i.e., the electrical resistivity and Seebeck coefficient) was determined from room temperature to 900 K in a nitrogen atmosphere using a four-probe method.

3. Results and discussion

Table 1 lists the Sb content and thickness of the deposited films. Fig. 1 shows XRD patterns of the Co–Sb thin films. CoSb$_3$ films have been reported to undergo transition from amorphous to polycrystalline at temperatures in the range 140–180 °C [16]. For this reason, we carried out deposition at 200 °C to obtain polycrystalline films. In the XRD patterns shown in Fig. 1, the different peaks indicate different grain orientations or secondary phases. Phase identification from the XRD peaks shows that the film deposited with an RF power of 40 W

Table 1
Composition, thickness and room-temperature Hall measurement data for as-deposited thin films obtained at each sputtering power.

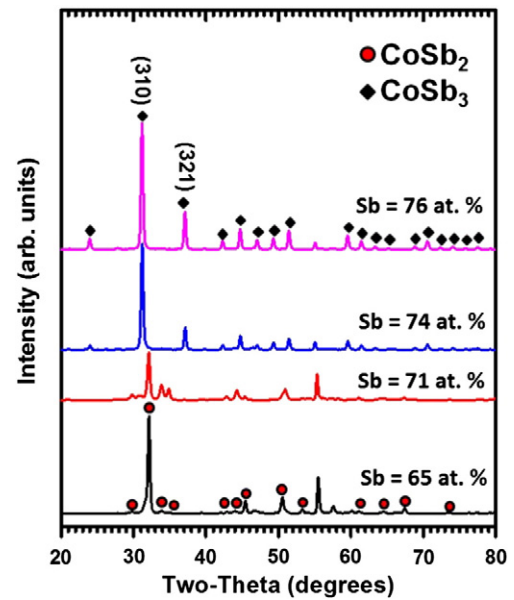| Sb target RF power (W)	Sb content (at. %)	Thickness (nm)	Bulk conc. (10^{19} cm^{-3})	Resistivity (μΩ·m)	Mobility (cm^2/V.s)
40	65	412	63.2	9.01	11.1
45	71	504	81	28.8	3.6
50	74	520	10.5	193	3.10
55	76	577	2.08	659	4.65

Fig. 1. X-ray diffraction patterns for the as-deposited films.

(with an atomic fraction of Sb of 65%), resulted in a CoSb$_2$ phase with a monoclinic crystalline structure. Increasing the sputtering power resulted in an increased Sb content. This is expected to result in a decreased quantity of CoSb$_2$ and the formation of more of the cubic, polycrystalline CoSb$_3$ skutterudite phase. The deposited film with an RF power of 45 W (71% Sb) exhibited CoSb$_2$ and CoSb$_3$ phases, with CoSb$_2$ as the dominant phase, as determined from the higher XRD peak intensities. Further increasing the Sb content resulted in single-phase CoSb$_3$ skutterudite thin films (with RF powers of 50 W and 55 W). Traces of CoSb$_2$ were still observed in XRD patterns of the former case, however. The skutterudite I(310) and I(321) XRD peaks of with an RF power of 55 W were higher than with 50 W, which is attributed to the larger Sb content.

Fig. 2 shows SEM images of the surface morphology. These indicate a well-defined grain structure, which confirms the polycrystalline nature of the films. The grain size depended on the Sb content, and therefore on the phase composition. The grain size was in the range 100–250 nm, and was found to be larger in the films where CoSb$_3$ was the dominant phase. Fig. 3 shows cross-sectional SEM images, which show a columnar grain structure.

Table 1 also lists the results of the Hall measurements on the thin films at the room temperature. All the as-deposited films exhibited p-type electrical behavior. The electrical resistivity can be expressed as follows:

$$\rho = \frac{1}{\sigma} = \frac{1}{ne\mu} \tag{2}$$

where σ is the electrical conductivity, n is the charge carrier concentration, e is the electronic charge and μ is the charge carrier mobility.

Note that the charge carrier concentration and the Hall mobility values for the CoSb$_3$ thin films were smaller than those for films with CoSb$_2$ as the dominant phase. This may be the reason that CoSb$_2$ thin films exhibited a resistivity that was close to that for a metal, whereas the resistivity of CoSb$_3$ films at room temperature was similar to that for semiconductors. While investigating the effect of the Sb content on the thermoelectric properties of bulk CoSb$_3$, Liu et al. showed that the band gap varied as a function of the Sb content [11]. More importantly, the band gap of CoSb$_3$ close to the stoichiometric ratio was significantly larger than that for films with a smaller Sb content. CoSb$_2$ has a much smaller band gap than CoSb$_3$, which explains the larger charge carrier concentration in the CoSb$_2$ films. The presence of defects and/or